AIAA-94-1925

On the Spatial and Temporal Accuracy of Overset Grid Methods for Moving Body Problems

R. Meakin
Overset Methods, Inc.
Moffett Field, CA

12th AIAA Applied Aerodynamics Conference
June 20-22, 1994 / Colorado Springs, CO

On the Spatial and Temporal Accuracy of Overset Grid Methods for Moving Body Problems

Robert L. Meakin *
Overset Methods, Inc.
at NASA Ames Research Center M/S 258-1
Moffett Field, CA 94035-1000

Abstract

A study of numerical attributes peculiar to an overset grid approach to unsteady aerodynamics prediction is presented. Attention is focused on the effect of spatial error associated with interpolation of intergrid boundary conditions and temporal error associated with explicit update of intergrid boundary points on overall solution accuracy. A set of numerical experiments are used to verify whether, or not, the use of simple interpolation for intergrid boundary conditions degrades the formal accuracy of a conventional second-order flow solver, and to quantify the error associated with explicit updating of intergrid boundary points. Test conditions correspond to the transonic regime. The validity of the numerical results presented here are established by comparison with existing numerical results of documented accuracy, and by direct comparison with experimental results.

INTRODUCTION

Computation of unsteady viscous flows for geometrically complex bodies involving relative motion between component parts represents an important class of problems for which accurate methods of prediction are required. There are numerous applications of this type; launch vehicle staging, aircraft store separation, crew escape mechanisms, and helicopter rotor/body interaction. Present engineering tools are inadequate for risk-free analysis of this class of problems, and trial-and-error testing has become too expensive and time-consuming. Mature computational methods such as empirically-modified, three-dimensional panel codes and nonlinear potential methods have been applied to these problems, but have not been completely successful. Unsteady viscous flowfields involving moving shocks, vortical wakes, interference effects and body motion demand the most advanced computational techniques available.

Currently, the only viable high-order method of prediction for these problems is the so called Chimera[1], or overset grid approach. The approach involves the decomposition of problem geometry into a number of geometrically simple overlapping component grids. Grid components associated with moving bodies move with the bodies without stretching or distorting the grid system. The structure of individual grid components facilitates viscous boundary layer resolution, and the use of implicit time-integration algorithms which are not held to the prohibitively low time-step limits characteristic of explicit schemes.

It is reasonable to presume that a solution method that has been verified to accurately predict the flow dynamics for a given application would also provide an accurate prediction for a new application, providing that the new geometry and flow conditions do not vary widely from those of the verified point of reference. If this were not the case, there would be no point in using computational methods of prediction, since construction of the test article, or prototype, would always be needed to verify the correctness of the prediction. Overset grid methods have been applied to a wide variety of problems and flow regimes. Careful verification studies have been carried out for many non-moving body cases [2,3,4,5,6]. However, data sets are usually only complete enough to verify the correctness of surface pressure predictions, and verification of moving body problems is practically impossible except for ideal cases. Accordingly, verification of the predictive ability of overset grid methods is an ongoing process. Of course, this is true of methods for Computational Fluid Dynamics (CFD) in general.

The objective of the present work is to explore basic attributes peculiar to an overset grid approach as they relate to accuracy in predicting the unsteady aerodynamic fields in moving body problems. The formal solution accuracy of the basic Navier-Stokes solver employed here[7] will be taken as a given. Attention is focused on the effect of spatial error associated with interpolation of intergrid boundary conditions and temporal error associated with explicit update of intergrid boundary points on overall solution accuracy.

DISCUSSION

An overset grid discretization of the space about geometrically complex bodies is comprised of a system of overlapping body-fitted grids and topologically simple background grids. The body-fitted grids extend a relatively short distance from body surfaces and are overset

* Staff Scientist, Member AIAA

maintain formal solution accuracy. In practical applications, given a fixed number of grid points, it is not possible to provide grid resolution of sufficient density to guarantee that flow features will always be smoothly represented in the grid. If a conservative interpolation scheme (e.g., see reference [11]) is used at intergrid boundaries, the speed and structure of flow features (i.e., shocks, vortices, etc.) can be maintained through grid interfaces. However, lacking sufficient grid resolution, the accuracy of the solution cannot be ensured in any case. Hence, the issue with domain connectivity is not necessarily one of conservative versus nonconservative interpolation, but one of grid resolution.

If solution adaption is used to ensure smooth variation of dependent variables throughout the computational space of overset grid systems, the resulting solutions will accurately approximate the governing differential equations in all respects. This point is demonstrated in subsequent paragraphs of this paper via a set of numerical experiments. The method of solution adaption suggested here is that of oversetting fine grid components where flow gradients/error indicators are high, as opposed to resorting to point redistribution methods.

Steady Transonic Airfoil Examples

Consider the steady flow over a NACA 0012 airfoil at Mach 0.8 freestream conditions and 1.25° angle-of-attack. These conditions result in a strong shock on the airfoil upper surface, and a very weak shock on the lower surface (see Figure 2). This flow situation has been used as a benchmark test condition for an AGARD advisory report on inviscid flow field methods[12]. In order to use the AGARD results as a point of reference for the present discussion, inviscid conditions have been imposed here also. This simplification in no way diminishes this case as a test of the effect of intergrid interpolation on solution accuracy.

The approach here is to carry out a grid refinement study and observe the rate at which the numerical error tends to zero. The error should decay at a second order rate since both the interior differencing scheme of the flow solver and the intergrid boundary interpolation scheme are second order. In order to correctly determine the numerical error associated with the present overset grid solutions, the exact Euler solution must be available. Unfortunately, the exact solution is unknown. Therefore, the single very fine grid solution shown in Figure 2 is used in lieu of the exact solution. The single very fine grid solution is referred to hereafter as STA-S-1 (**S**teady **T**ransonic **A**irfoil - **S**ingle grid - case **1**).

The STA-S-1 solution was obtained using 643 points in the azimuthal direction (J), and 131 points in the surface normal direction (K). Since the flow solver used here is fully 3D, the present 2D problem was simulated using 3 planes of 643×131 points. This spacing is twice that of the finest AGARD solution. In addition to STA-S-1, four overset grid solutions of the same problem were carried out using grids of varying resolution. The naming convention adopted for the overset grid solutions is STA-M-X. The "M" stands for multiple grid case, and "X" stands for the particular case number referenced in Table 1. Table 1 gives statistics of the grid systems for each case presented in this section.

The overset grids are each composed of a body-fitted grid for the airfoil, and a background Cartesian grid of corresponding resolution. The body-fitted grids are each subsets of STA-S-1. For example, STA-M-1 is identical with STA-S-1 for all points in J and all points in K out to K = 61. STA-M-2 was obtained by using every other point from STA-M-1 in both the J and K directions. STA-M-3 was obtained by using every third point in J and K. STA-M-4 was obtained by using every sixth point in J and K. Since all overset grids have points in common with STA-S-1, the point-wise numerical error in each overset solution can be computed as a simple difference with the STA-S-1 solution. Figure 3 shows a plot matrix of the error which resulted on each overset grid solution. The top row shows solution error in the coarse overset solution (STA-M-4) with respect to the single very fine grid solution (STA-S-1). Moving from top-to-bottom, the error plots correspond to increasingly fine overset grid solutions. The first column of plots in Figure 3 is the local error in mass density. The second and third columns are the local error in X-momentum and total energy, respectively. Figure 4 shows the rate at which the error decays as a function of grid resolution. The error represented in Figure 4 is the rms error of the error fields shown in Figure 3. The solid lines shown in Figure 4 represent first and second order slopes (i.e., 2nd order implies that doubling the number of grid points will reduce the error by a factor of 4).

The error reduction from the STA-M-4 to STA-M-3 solutions is second order in all flow variables. This is also true for the scalar variables (ρ and e) throughout the range of grid refinement. However, the vector variables (ρU and ρW) drop to a nearly first order slope between the STA-M-3 and STA-M-2 solutions. The reason for this is that the reference solution (STA-S-1) is not exact. As the resolution of the overset grids approaches that of the reference STA-S-1 case, the error computations become invalid.

Surface C_p plots are presented in Figures 5 and 6. Figure 5 provides a comparison with the finest AGARD solution and the present STA-S-1 and STA-M-1 solutions. Clearly, the three solutions are in very good agreement. Figure 6 provides a comparison with the finest AGARD solution (again) and two relatively coarse-grid solutions,

fully implicit, a temporal error will result. Full aircraft applications can involve as many as 100 grid components, perhaps more. At what point does the temporal error associated with explicit intergrid boundary updates become significant? The second concern relates to numerical stability. As a domain is decomposed into more and more grid components, the lagging of intergrid boundaries makes the overall solution procedure more explicit. Indeed, in the limit as the domain is decomposed into as many grid components as there are grid points, the scheme is reduced (in essence) to Point Jacobi. At what point, then, does stability become a real issue?

Unsteady Transonic Oscillating Airfoil Examples

In order to explore the questions posed above, consider the case of an oscillating airfoil subject to transonic flow conditions. Specifically, consider a NACA 64A010 airfoil subject to Mach 0.796 freestream conditions and forced oscillation of constant amplitude. The specific case to be considered here is defined in Table 3, and results in an attached boundary layer and weak moving upper and lower surface shocks. The motion of the shocks, and unsteady aerodynamic loads are driven by the amplitude and frequency of oscillation of the airfoil. As with the steady-state cases considered previously, the approach here is to determine numerical error relative to a very fine benchmark solution. The benchmark solution is referred to as UTOA-S-1 (**U**nsteady **T**ransonic **O**scillating **A**irfoil - **S**ingle grid - case **1**). Like the STA-S-1 case of the previous section, the UTOA-S-1 grid has 643 points in the azimuthal direction (J), and 131 points in the surface normal direction (K) (see Figure 10). Relative to a dimensionless chord length of unity, the initial spacing away from the wall is 1×10^{-6}.

In order to isolate the error and stability concerns attributable to the explicit updating of intergrid boundary points, the UTOA-S-1 grid was decomposed in a special way to form the basis for the five multiple grid computational cases indicated in Table 4 (note that the "M" in Table 4 nomenclature indicates Multiple grid case). For example, the UTOA-S-1 grid was decomposed into the two overlapping grids indicated in Figure 10 (UTOA-M-1). Both grid components in the UTOA-M-1 grid are exact subsets of the UTOA-S-1 grid. Intergrid boundary points in the inner UTOA-M-1 grid are coincident with interior points of the outer UTOA-M-1 grid. Likewise, intergrid boundary points on the outer UTOA-M-1 grid are coincident with interior points of the inner UTOA-M-1 grid. As a result, there is no interpolation error associated with intergrid boundary condition updates. Further, the procedure is spatially conservative. The only possible source of error in the computations, relative to the UTOA-S-1 benchmark solution, is the explicit nature of the intergrid boundary updating procedure.

Adopting the same method of decomposition used to realize the 2 component UTOA-M-1 grid system, the UTOA-S-1 grid was decomposed into grid systems with 16 and 32 components (see Figure 10). The 16 component grid system corresponds to the UTOA-M-2 case indicated in Table 4. The 32 component grid system corresponds to the UTOA-M-3, UTOA-M-4, and UTOA-M-5 cases indicated in Table 4. Cases UTOA-M-1 through UTOA-M-3 correspond to simulations using the same time-step size as that employed in UTOA-S-1, and allow the temporal error resulting from explicit intergrid updating to be identified. Cases UTOA-M-3 through UTOA-M-5 correspond to simulations carried out on the 32 component grid system for time-step sizes of $\Delta t = 0.0025$, $2 \times \Delta t$, and $4 \times \Delta t$, respectively. As a result, cases UTOA-M-3 through UTOA-M-5 may furnish some insight into the impact on stability of explicit intergrid boundary updates.

The physical problem being solved in all the UTOA cases indicated in Table 4 has been studied experimentally in the NASA Ames 11 x 11 foot wind-tunnel[13]. An attempt to verify the validity of the benchmark case by comparison with experiment has been carried out. However, due to circumstances outlined below, the experimental data set employed did not facilitate a conclusive solution validation comparison. This not withstanding, the UTOA cases do provide important reference information regarding the numerical questions immediately at hand.

The benchmark UTOA-S-1 unsteady solution was initiated from a nearly converged static (non-oscillating) solution about the airfoil at mean angle-of-attack ($\alpha_m = -0.21°$). The surface C_p distribution resulting from a fully converged static airfoil case is shown in Figure 11, along with the experimental results. The agreement between the computation and experiment is very good. However, there is a slight discrepancy in C_p magnitude over the first 40% chord of the foil. The reason for this is that the foil geometry used in the computation is based on the OSU definition of a NACA 64A010[14], rather than the coordinates published in reference[13]. Figure 12 illustrates the differences in the theoretical, experimental, and OSU definitions of the NACA 64A010 geometry. The definition used in the computations (OSU) corresponds to the theoretical definition up to about 50% chord and then smoothly transitions to the experimental definition. Figure 11 also contains a full potential solution to this problem based on the theoretical NACA 64A010 definition. The full potential solution was provided for comparative purposes only. The computed integral loads (C_l and C_m) are in good agreement with the corresponding experimental results (see tabu-

crepancies between experiment and computed solutions obtained using an overset grid approach. The present results suggest that grid resolution is the primary issue. If it is not possible to provide sufficient grid resolution for a given problem, a conservative interface scheme is preferable, but accuracy will be compromised whether, or not, conservation has been maintained across grid interfaces. The present study suggests the use of overset fine grids as a practical means of insuring smooth representation of flow gradients in overset grid systems, and hence, maximizing solution accuracy.

The steady state STA-M grid refinement study carried out here indicates that formal solution accuracy is maintained in an overset grid system using tri-linear interpolation to supply intergrid boundary conditions. The results confirm that spatial error associated with interpolation of intergrid boundary data can be minimized via overset fine grid components. This appears to be true even if grid interfaces exist across shocks.

Explicit updating of intergrid boundary conditions did not have a significant adverse affect on solution accuracy for the present UTOA cases, for which the solution domain was split into as many as 32 overlapping grid components. Solution error attributable to explicit updating of intergrid boundaries was observed to be proportional to the time-step size employed, however remained insignificant for all stable Δt. The present UTOA-M cases inherited no discernible stability penalties as a result of the explicit intergrid boundary updates. These results suggest that unsteady problems of practical importance (3D complex geometry) can be accurately simulated using an overset grid approach provided that the time-step size is sufficient to resolve the significant temporal gradients inherent to the problem.

ACKNOWLEDGEMENTS:

This work was carried out under NASA ARC grant NCC2-747. All computational results reported herein were carried out on the NAS facility at NASA ARC. The author wishes to acknowledge the influence of the late Professor Joseph Steger on this work, as well as the author's present course of research. In addition, thanks are due to Drs. Kalpana Chawla and Christopher Atwood who have been very encouraging and have always been available for discussions on the issues presented herein. The support and direction provided by Dr. Jim McCroskey is also gratefully acknowledged.

REFERENCES

[1] Steger, J. L., Dougherty, F. C., and Benek, J. A., "A Chimera Grid Scheme," Advances in Grid Generation, K. N. Ghia and U. Ghia, eds., ASME FED-Vol 5., June 1983.

[2] Martin, F. and Slotnick, J., "Flow Computations for the Space Shuttle in Ascent Mode Using Thin-Layer Navier-Stokes Equations," Progress in Astronautics and Aeronautics, Vol. 125: Applied Computational Aerodynamics, P. Henne, Ed., AIAA, 1990.

[3] Meakin, R., "Computations of the Unsteady Flow About a Generic Wing/Pylon/Finned-Store Configuration," AIAA Paper 92-4568-CP, pp. 564-580, August 1992.

[4] Lijewski, L. and Suhs, N., "Chimera-Eagle Store Separation," AIAA Paper 92-4569, August, 1992.

[5] Jordan, J., "Computational Investigation of Predicted Store Loads in Mutual Interference Flow Fields," AIAA Paper 92-4570-CP, pp. 581-591, August, 1992.

[6] Benek, J., Donegan, T., and Suhs, N., "Extended Chimera Grid Embedding Scheme with Application to Viscous Flows," AIAA Paper 87-1126-CP, pp. 283-291, 1987.

[7] Renze, K., Buning, P., and Rajagoplan, R., "A Comparative Study of Turbulence Models for Overset Grids," AIAA Paper 92-0437, January, 1992.

[8] Meakin, R., "A New Method For Establishing Inter-Grid Communication Among Systems of Overset Grids," AIAA Paper 91-1586-CP, pp. 662-671, June, 1991.

[9] Dietz, W., Jacocks, J., and Fox, J., "Application of Domain Decomposition to the Analysis of Complex Aerodynamic Configurations," SIAM Conf. Domain Decomposition Meths., Houston, TX, March 1989.

[10] Brown, D., Chesshire, G., Henshaw, W., and Kreiss, O., "On Composite Overlapping Grids," 7th Internat. Conf. on Finite Element Methods in Flow Problems, Huntsville, AL, April 1989.

[11] Moon, Y. and Liou, M., "Conservative Treatment of Boundary Interfaces for Overlaid Grids and Multilevel Grid Adaptions," AIAA Paper 89-1980-CP, pp. 480-494, 1989.

[12] Viviand, H., "Numerical Solutions of Two- Dimensional Reference Test Cases," AGARD-AR-211: Test Cases for Inviscid Flow Field Methods.

[13] Davis, S. and Malcolm, G., "Experimental Unsteady Aerodynamics of Conventional and Supercritical Airfoils," NASA TM-81221, August, 1980.

[14] Olsen, J., "AGARD Standard Configurations for Aeroelastic Applications of Transonic Unsteady Aerodynamics," AFFDL-TM-78-6-FBR, Part III (Addendum), October, 1978.

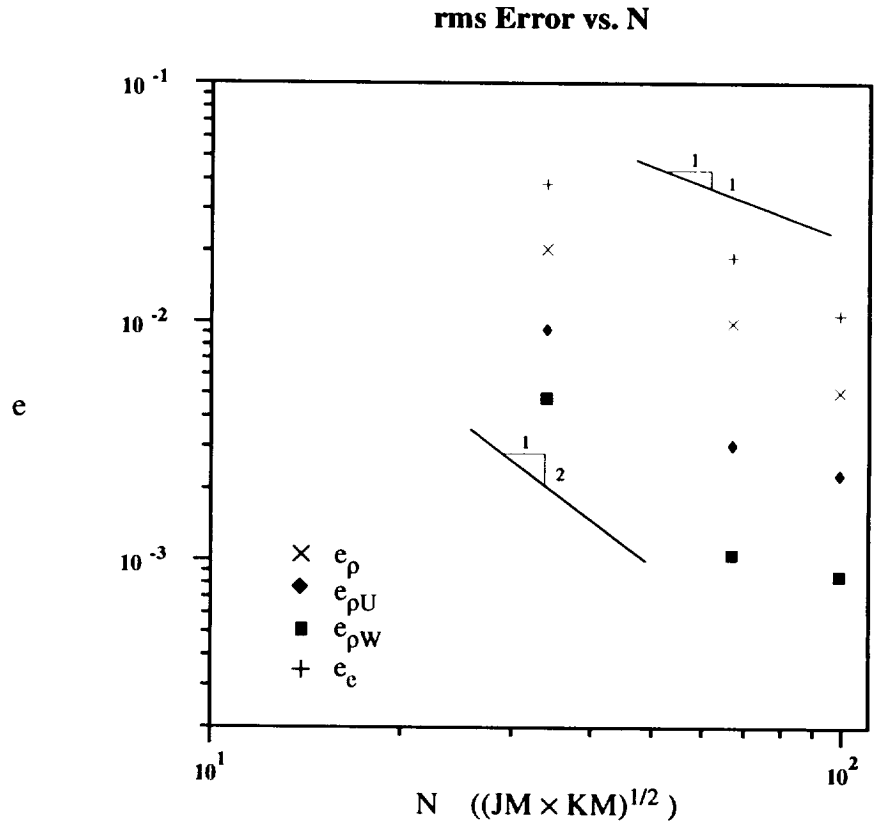

Figure 4. Grid refinement and rms error reduction for STA cases.

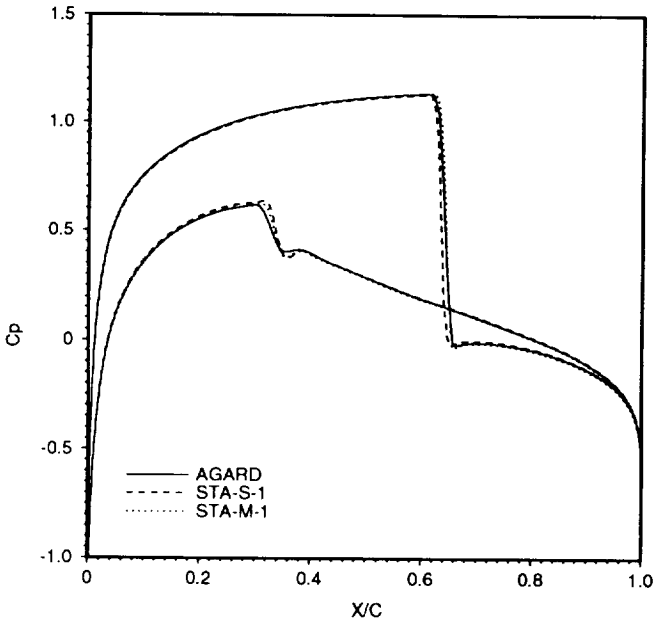

Figure 5. C_p vs. X/C plots for the finest AGARD solution [12], and the present STA-S-1 and STA-M-1 solutions.

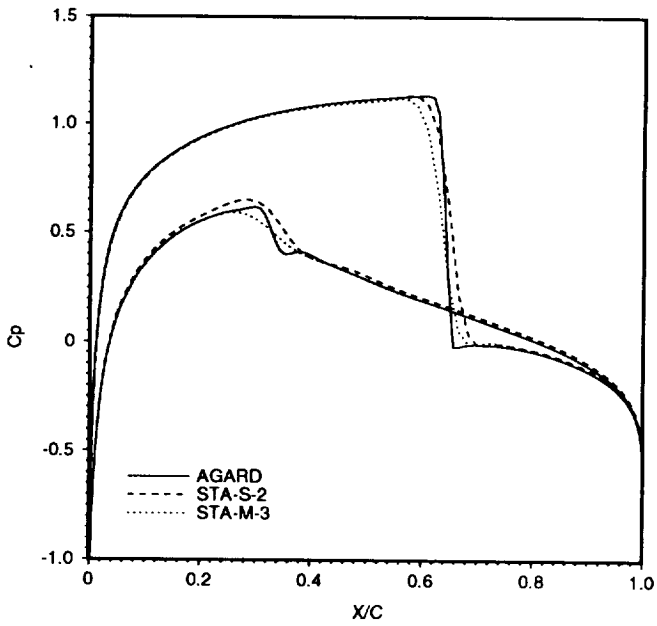

Figure 6. C_p vs. X/C plots for the finest AGARD solution [12], and the present coarse STA-S-2 and STA-M-3 solutions.

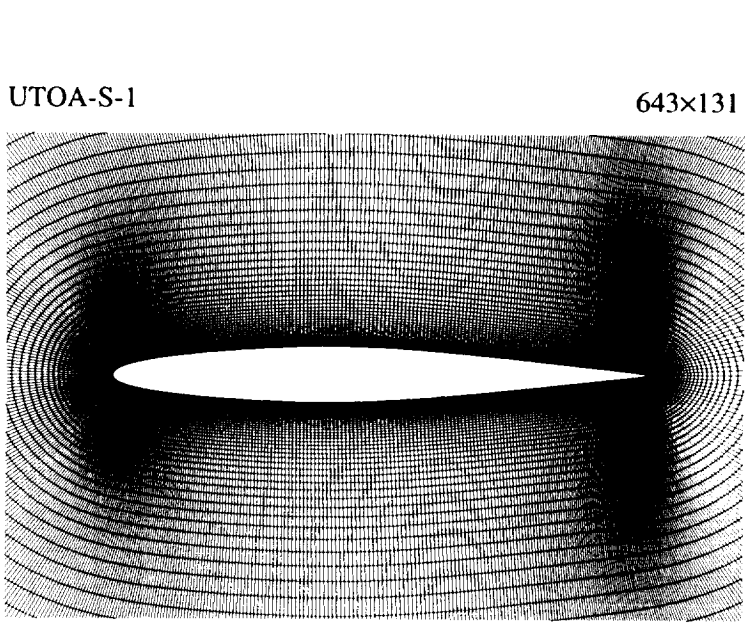

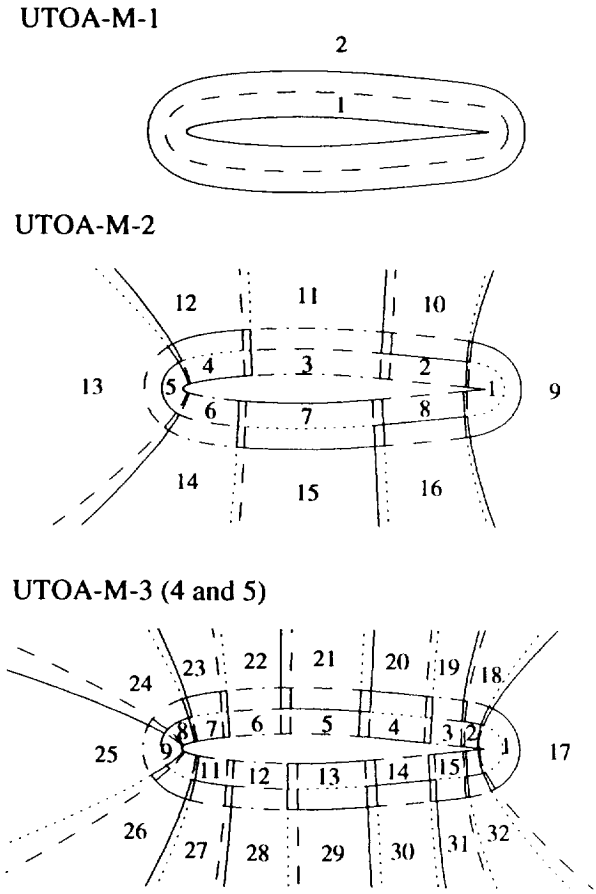

Figure 10. Decomposition of the UTOA-S-1 grid into 2, 16, and 32 overlapping grid components. Intergrid boundary conditions are spatially conservative and have no interpolation error.

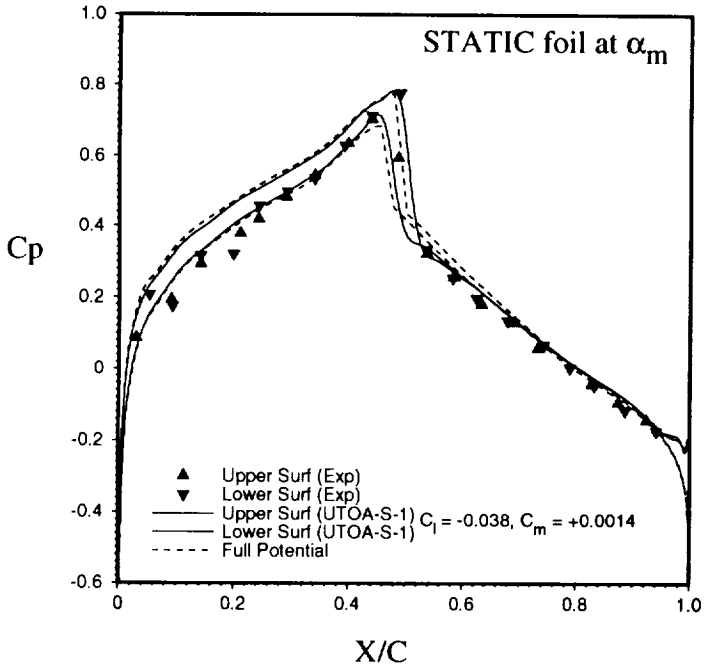

Figure 11. Cp vs X/C comparison between NASA Experiment [13], the present UTOA-S-1 solution, and, for reference, a Full Potential solution ($M_\infty = 0.796$, $\alpha_m = -0.21^o$, $Re = 1.256 \times 10^7$).

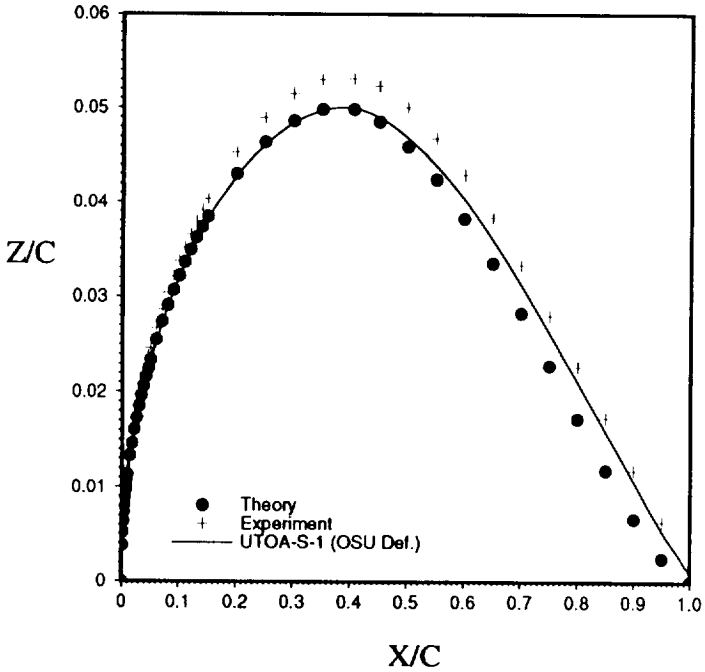

Figure 12. NACA 64A010 airfoil definitions. a) Theoretical coordinates presented in [13], b) coordinates of experimental configuration [13], and c) coordinates used in UTOA computations (based on OSU definition[14]).

Table 1. Grid Refinement Cases

Case[1]	Grids[2]	Type	JM x KM
AGARD	1	O	320 x 64
STA-S-1	1	O	643 x 131
STA-S-2	1	O	215 x 44
STA-M-1	2	O	643 x 61
		BC	309 x 195
STA-M-2	2	O	322 x 31
		BC	155 x 97
STA-M-3	2	O	215 x 21
		BC	103 x 65
STA-M-4	2	O	108 x 11
		BC	51 x 33
STA-AG	7	O	215 x 21
		BC	103 x 65
		FBF	25 x 21
		FBF	31 x 21
		FBF	37 x 17
		FBF	39 x 21
		FC	22 x 25

1 Outer boundary is 25 chords in all cases.

2 Type legend:
O = "O" topology
BC = Background Cartesian
FBF = Fine Body-Fitted
FC = Fine Cartesian

Table 2. Computed Loads

Case	C_D	C_L	C_M
AGARD	0.0230	0.3632	-0.0397
scatter*	±0.0023	±0.0273	±0.0072
STA-S-1	0.0145	0.3403	-0.0359
STA-M-1	0.0155	0.3569	-0.0394
STA-M-2	0.0148	0.3372	-0.0357
STA-M-3	0.0152	0.3463	-0.0361
STA-M-4	0.0195	0.3085	-0.0319
STA-AG	0.0162	0.3487	-0.0358

* Scatter given in AGARD report[12] is based on 9 Euler solutions to the present flow conditions from varying solvers, grid densities, and grid type.

Table 3. Unsteady Transonic Oscillating Airfoil (UTOA) Test Conditions

ID	55	NASA TM-81221* Case ID
Foil		NACA 64A010
M_∞	0.796	Free Stream Mach
R_e	12.56×10^6	Reynolds Number
α	$\alpha_o \cos(\omega t)$	Oscillatory angle of incidence
α_m	-0.21^o	Mean angle-of-attack
α_o	1.01^o	Oscillatory pitch amplitude
κ	0.202	Reduced frequency $\kappa = \omega l/2U$ $\omega = 2\pi f$
f	34.4	Frequency (Hz)
x_o/C	0.248	Pitch axis w/r leading edge
l	0.500	Chord length (m)
c_∞	336	Sonic speed (m/s)

* See reference [13]

Table 4. UTOA Test Cases

Case	Grids	Δt
UTOA-S-1	1	0.0025
UTOA-M-1	2	0.0025
UTOA-M-2	16	0.0025
UTOA-M-3	32	0.0025
UTOA-M-4	32	0.0050
UTOA-M-5	32	0.0100

Case UTOA-S-1 is the benchmark case.

Cases UTOA-M-1 through UTOA-M-5 are multiple grids cases which have zero interpolation error, and are fully conservative.